

# Structural studies of the main exopolysaccharide produced by the deep-sea bacterium *Alteromonas infernus*

Olivier Roger,<sup>a</sup> Nelly Kervarec,<sup>b</sup> Jacqueline Ratiskol,<sup>a</sup>  
Sylvia Collicec-Jouault<sup>a</sup> and Lionel Chevolot<sup>a,c,\*</sup>

<sup>a</sup>Laboratoire de Biotechnologie des Molécules Marines, IFREMER, Département Valorisation des Produits,  
BP 21105, F-44311 Nantes, France

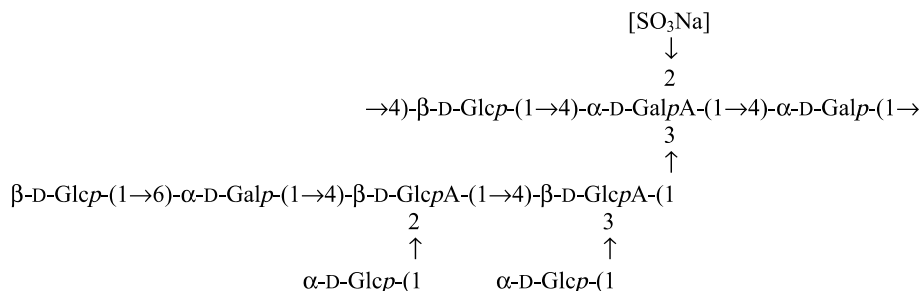
<sup>b</sup>Laboratoire de RMN, Université de Bretagne Occidentale, F-29200 Brest, France

<sup>c</sup>Laboratoire de Recherches sur les Macromolécules, CNRS/Université Paris 13, F-97354 Villetaneuse, France

Received 19 April 2004; received in revised form 28 July 2004; accepted 30 July 2004

Available online 9 September 2004

**Abstract**—The structure of the extracellular polysaccharide produced by the mesophilic species, *Alteromonas infernus*, found in deep-sea hydrothermal vents and grown under laboratory conditions, has been investigated using partial depolymerization, methylation analysis, mass spectrometry and NMR spectroscopy. The repeating units of this polysaccharide is a nonasaccharide with the following structure:



© 2004 Elsevier Ltd. All rights reserved.

**Keywords:** *Alteromonas*; Bacterial polysaccharide; Structure; Hydrothermal vent

## 1. Introduction

Marine microorganisms, present near deep-sea hydrothermal vents, have been studied for several years because they grow in very exceptional conditions characterized by extreme pressures and temperature and high concentration of toxic elements. Several bacteria (e.g., *Alteromonas macleodii* subsp. *fijiensis* and

*Vibrio diabolicus*) found in such environments produce extracellular polymers with unusual structures, when grown aerobically in a carbohydrate-based medium.<sup>1,2</sup> Such polysaccharides were first studied for their rheological properties or metal complexing abilities.<sup>3,4</sup> However, in the last few years, scientific interest for the biological activities (especially heparin-like) of microbial polysaccharides has increased.

In this context, we have started to study the polysaccharide produced by *Alteromonas infernus*, a new species of bacterium<sup>5</sup> classified as a nonpathogenic microorganism by the Institut Pasteur. It secretes a water-soluble

\* Corresponding author at present address: UPS CNRS 2561, 16 rue A. Aron, F-97300 Cayenne, French Guiana. E-mail: [lionel.chevolot@guyane.cnrs.fr](mailto:lionel.chevolot@guyane.cnrs.fr)

acidic exopolysaccharide (EPS) consisting mainly of glucose, galactose, glucuronic and galacturonic acids with variable amounts of rhamnose. This high-molecular-weight polysaccharide ( $10^6$  g/mol) differs in both its monosaccharide and sulfate content (10%) from other EPS produced by deep-sea hydrothermal bacteria and from polysaccharides of other origins. The native EPS secreted by *A. infernus* does not possess anticoagulant activity. Nevertheless, several oversulfated low-molecular-weight EPS fractions (sulfated LMW-EPS), with uronic acid and sulfate contents comparable to those of heparin, have been prepared by partial hydrolysis and chemical sulfation;<sup>6</sup> some of these fractions displayed interesting anticoagulant activity.<sup>7</sup> They were less potent than low-molecular-weight heparin and unfractionated heparin in activated partial thromboplastin time (APTT) assays (2.5 and 6.5 times, respectively), but more potent than LMW dermatan sulfate.<sup>8</sup> Affinity co-electrophoresis experiments performed in the presence of antithrombin or heparin co-factor II showed that all chains of sulfated LMW-EPS bound antithrombin strongly while only a subpopulation did the same with heparin co-factor II.<sup>7</sup> This latter result strongly suggests that the anticoagulant activity is modulated not only by the sulfate content, but also by the position of sulfate groups along the polysaccharide chain.

In a previous paper,<sup>7</sup> methylation analysis data (with or without reduction) of the crude EPS were described. They indicated the presence of 11 different residues and of three side chains terminated by a Glcp or a Galp, the branched residues being a 3,4-disubstituted GalpA, a 3,4-disubstituted GlcpA and a 2,4-disubstituted GlcpA. The present report provides the complete structural determination of the *A. infernus* EPS.

## 2. Results and discussion

### 2.1. Native EPS

A crude preparation of EPS was obtained by precipitation and ultrafiltration as previously described.<sup>6</sup> Compositional and methylation analyses (see Table 1) gave the same results as those previously reported. It can be underlined that sugar ratios were not stoichiometric and that the presence of some residues (like  $[\rightarrow 3]\text{-Rhap-(1}\rightarrow)]$  or  $[\text{Galp-(1}\rightarrow)]$  was not consistent with the proposed structure. Several hypotheses (nonexclusive) should explain this discrepancy: degradation occurring during the extraction process (loss of some terminal sugars) or during the methylation reaction, incomplete reduction of uronic acids, presence of more than one polysaccharide in the native EPS (see below). Determination of the absolute configurations indicated that rhamnose has the L-configuration, whereas glucose, galactose, glucuronic and galacturonic acids have the D-configuration. NMR spectra of the native EPS displayed very poor resolution owing to its high MW and, therefore, they are not discussed. Consequently, NMR studies were carried out with two lower-MW fractions obtained by partial hydrolysis (see below).

### 2.2. Preparation, purification and structure determination of the oligosaccharide fraction (OF)

A fraction containing only small oligosaccharides (called OF in the following) was prepared by acid hydrolysis followed by ultrafiltration through a 1000 Da membrane. An aliquot of this fraction was also reduced by  $\text{NaBH}_4$  (rOF). Analysis of partially methyl-

**Table 1.** Analysis of methylated and carboxyl reduced polysaccharide alditol acetates of *A. infernus* strain exopolysaccharide (native EPS), oligosaccharide fraction (fraction OF) and gently hydrolyzed EPS (LMW-EPS)

PMAA <sup>a</sup>	$t_R^b$	Detector response (%)			Deduced linkage
		Native EPS	Fraction OF	LMW-EPS	
2,4,6-Me <sub>3</sub> Rha <sup>c</sup>	0.69	8.1	Tr <sup>e</sup>	Tr <sup>e</sup>	$\rightarrow 3\text{-Rhap-(1}\rightarrow)$
2,3,4,6-Me <sub>4</sub> Glc	0.71	19.3	22	21	Glcp-(1 $\rightarrow$
2,3,4,6-Me <sub>4</sub> Gal	0.73	8.0	0	7	Galp-(1 $\rightarrow$
2,3,6-Me <sub>3</sub> Gal	0.79	14.3	8.0	7	$\rightarrow 4\text{-Galp-(1}\rightarrow$
2,3,6-Me <sub>3</sub> Glc	0.80	10.3	0	8	$\rightarrow 4\text{-Glcp-(1}\rightarrow$
2,3,4-Me <sub>3</sub> Glc-6- $d_2^d$	0.82	4.0	29	0	GlcpA-(1 $\rightarrow$
2,3,4-Me <sub>3</sub> Gal	0.85	6.7	0	2	$\rightarrow 6\text{-Galp-(1}\rightarrow$
2,3-Me <sub>2</sub> Glc-6- $d_2$	0.90	10.3	22	9	$\rightarrow 4\text{-GlcpA-(1}\rightarrow$
2,4-Me <sub>2</sub> Glc-6- $d_2$	0.93		4	0	$\rightarrow 3\text{-GalpA-(1}\rightarrow$
2-MeGlc-6- $d_2$	0.95	5.3	0	8	$\rightarrow 3,4\text{-GlcpA-(1}\rightarrow$
2-MeGal-6- $d_2$	0.96	4.0	2	9	$\rightarrow 3,4\text{-GalpA-(1}\rightarrow$
3-MeGlc-6- $d_2$	0.97	4.1	0	4	$\rightarrow 2,4\text{-GlcpA-(1}\rightarrow$

<sup>a</sup> PMAA: Partially methylated alditol acetate.

<sup>b</sup>  $t_R$  = Retention time for the corresponding alditol acetate relative to that of *myo*-inositol hexaacetate ( $t_R = 1.000$ ).

<sup>c</sup> 2,4,6-Me<sub>3</sub>Rha = 1,3,5-tri-*O*-acetyl-2,4,6-tri-*O*-methyl-rhamnitol, etc.

<sup>d</sup> 2,3,4-Me<sub>3</sub>Glc-6- $d_2$  = 1,5,6-tri-*O*-acetyl-6,6-dideutero-2,3,4-tri-*O*-methylglucitol.

<sup>e</sup> Tr = trace (less than 2%).

ated alditol acetates (PMAA) prepared from OF (see Table 1) showed the presence of six different residues, three being much more abundant and corresponding to unsubstituted Glcp, unsubstituted GlcpA and 4-substituted GlcpA. The three others were due to 3,4-disubstituted GalpA, 3-substituted GalpA and 4-substituted Galp. OF contained only traces of Rha.

**2.2.1. ESIMS studies of the reduced oligosaccharide fraction (rOF).** The rOF fraction was then analyzed by mass spectrometry with electrospray ionization (ESIMS) in the negative mode. The results (Table 2) established the presence of four different oligosaccharides. The peaks at  $m/z$  951 and 973 (sodium form) corresponded to a mono-sulfated reduced pentasaccharide containing two hexose residues and three uronic acids. Doubly charged ions were also detected ( $m/z$  475 and 486). A second series of peaks at 80 ( $m/z$  871 and 893) or 40  $m/z$  less ( $m/z$  435, 446 for doubly charged ions) corresponded to the same pentasaccharide, but with no sulfate group. The mass difference between the sulfated pentasaccharide and the ion at  $m/z$  at 789 was 162. This represents a neutral dehydrated hexose (180–18) such as glucose or galactose. Consequently, the ion at  $m/z$  789 was generated by a reduced sulfated tetrasaccharide. The corresponding unsulfated tetrasaccharide appeared at  $m/z$  709. MS/MS experiments were performed on the most abundant ion at  $m/z$  871 (unsulfated pentasaccharide). The fragmentation pattern is shown in Figure 1.

The results indicated the presence of a trisubstituted HexA, bearing a hexitol residue and two nonreducing end terminals, one constituted of a hexose residue and the other one by the disaccharide HexA-HexA. Combining these results with those deduced from the PMAA experiments, the partial structure of the reduced unsulfated pentasaccharide is: [GlcA-(1→4)-GlcA-(1→3)[Glc-(1→4)]-GalpA-(1→?)-hexitol]. The loss of the terminal Glc-(1→4) residue gave the tetrasaccharides. It should be underlined that the PMAAs corresponding to the [ $\rightarrow$ 3,4)-GalpA] and [ $\rightarrow$ 3,4)-GalpA-(2SO<sub>3</sub><sup>−</sup>)-(1→)] were detected in very low amounts or were totally absent. Several hypotheses may explain this result. GalA residues might be destroyed (in part or totally) by  $\beta$ -elimination, under the basic conditions used for the methylation. Yang and Montgomery<sup>9</sup> reported such decomposition during the methylation of a polysaccharide containing a 4-linked glucuronic acid. Rougeaux et al.<sup>1</sup> obtained also, in low yield, the PMAA corresponding to [ $\rightarrow$ 3,4)-GalpA] in their study of the *A. macloidii* polysaccharide. On the other hand, 2-sulfated galacturonic acid was not detected because sulfate ion (a good leaving group) was certainly removed by elimination or substitution. Finally, ‘peeling reaction’ as well as incomplete reduction of the carboxylic function could also explain this result.

**2.2.2. NMR spectral studies of OF.** In the anomeric region of the <sup>1</sup>H spectrum of OF, several peaks appeared between 4.5 and 5.32 ppm, but some were not due to

**Table 2.** Negative-ion mode ESIMS analysis of the NaBH<sub>4</sub> reduced oligosaccharide fraction (rOF)

Oligosaccharide	$m/z$ , Assignment			
	$[M-H]^-$	$[M-2H+Na]^-$	$[M-2H]^{2-}/2$	$[M-3H+Na]^{2-}/2$
Sulfated pentasaccharide	951	973	475	486
Pentasaccharide	871	893	435	446
Sulfated tetrasaccharide	789	—	—	405
Tetrasaccharide	709	731	—	365

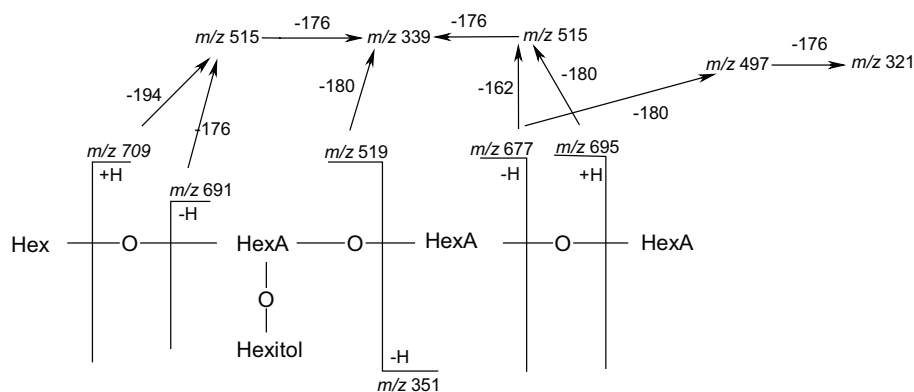


**Figure 1.** MS/MS fragmentation pattern of the precursor ion  $m/z$  871  $[M-H]^-$ . This ion was the most important observed in ESIMS of the reduced fraction rOF in negative mode. Abbreviations are Hex for Glcp or Galp, HexA for GlcA or GalA while hexitol is the reduced terminal residue.

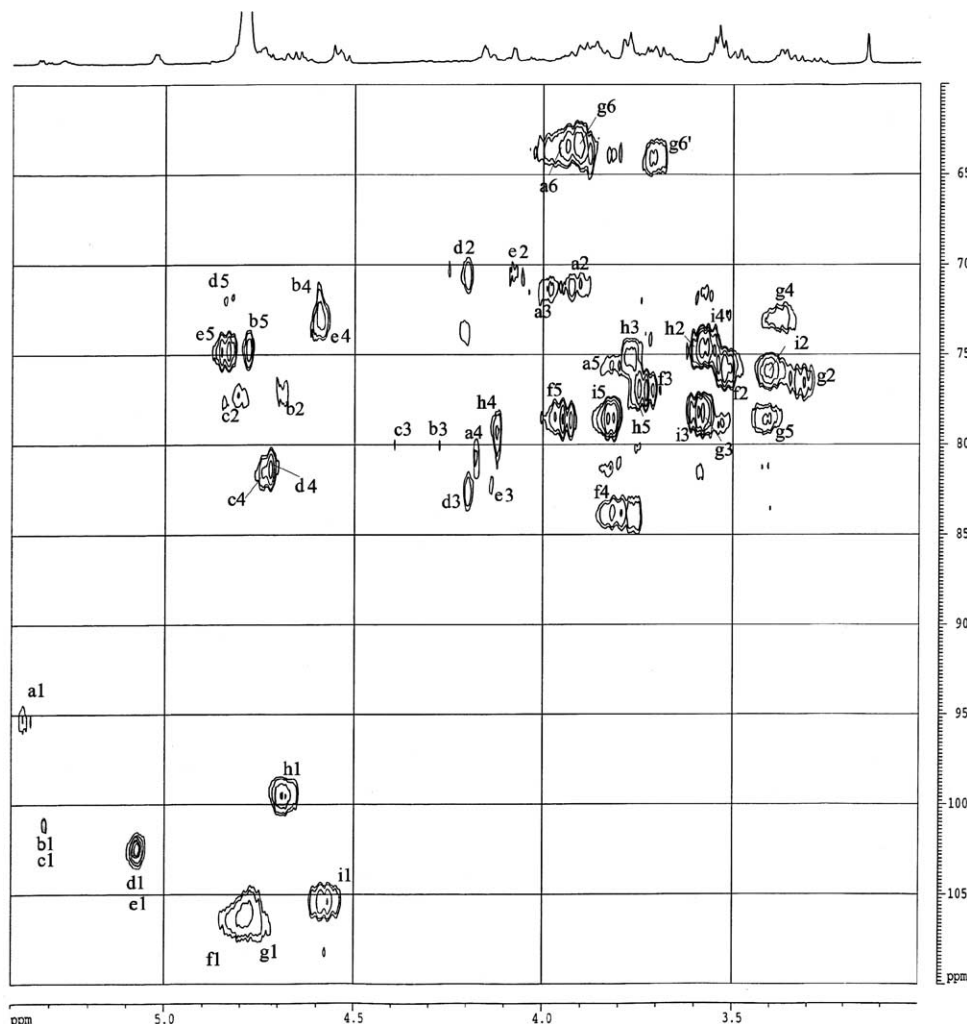


**Figure 2.** HSQC spectrum (500 MHz) of oligosaccharides (OF fraction) recorded at 325 K in deuterium oxide.

anomeric protons, as shown by the HSQC spectrum (Fig. 2), which contained cross-peaks outside the  $^{13}\text{C}$  region of anomeric signals. This spectrum displayed seven H-1/C-1 cross-peaks corresponding to nine different residues: five  $\alpha$ -linked (**a**–**e**) and four  $\beta$ -linked (**f**–**i**), as deduced from the chemical shifts of the C-1 and H-1. DQF-COSY, TOCSY and HSQC experiments were performed to assign almost all  $^1\text{H}$  and  $^{13}\text{C}$  resonances of each sugar (Table 3). Residues **a** and **h** corresponded to the reducing end (in  $\alpha$  and  $\beta$  form, respectively). The chemical shifts of H-2 (at  $\delta$  3.87 and 3.56), H-3 (at  $\delta$  3.95 and 3.73) and H-4 (at  $\delta$  4.14 and 4.08) of both residues were in agreement with sugars of the *galacto* series. The downfield chemical shifts of C-4 ( $\delta$  81.0 and  $\delta$  79.2) indicated that **a** and **h** were 4-substituted. Both series of signals disappeared after  $\text{NaBH}_4$  reduction, which confirmed these attributions.

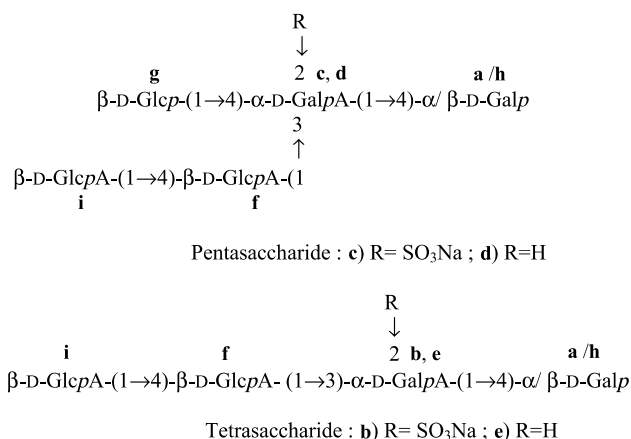
The H-3/H-4 cross-peaks, in the COSY spectrum of **b** and **c**, displayed the characteristic shape of *galacto* residues (due to the small coupling constants of H-4 with H-3 and H-5). The downfield chemical shifts of H-4 (see

Table 3) were consistent with a galacturonic acid structure.<sup>1</sup> The particularly downfield chemical shifts of H-2 established that position 2 of these residues bore a sulfate group. The C-3 at  $\delta$  80.0 for **b** and **c** and C-4 at  $\delta$  81.5 for **c** indicated that residue **b** was 3-substituted and **c** was 3,4-disubstituted. Consequently, **b** and **c** were  $[\rightarrow 3)\text{-}\alpha\text{-D-GalpA}-(2\text{SO}_3^-)-(1\rightarrow]$  and  $[\rightarrow 3,4)\text{-}\alpha\text{-D-GalpA}-(2\text{SO}_3^-)-(1\rightarrow]$ , respectively. Residues **d** and **e** were very similar to **c** and **b**, respectively, except for H-2. The H-2 resonances at  $\delta$  4.17 (**d**) and 4.03 (**e**) indicated that no sulfate group was present on those residues, **d** was identified as a 3,4-disubstituted- $\alpha\text{-D-GalpA}$  and **e** as a 3-monosubstituted- $\alpha\text{-D-GalpA}$ . In fact, **b**, **d** and **e** were the various possible residues generated by partial hydrolysis from the same initial unit **c**.

The  $\beta$ -*gluco* configuration assigned to the residues **f**, **g** and **i**, was in complete agreement with the upfield positions of H-1 and H-2. The chemical shift of C-4 of residue **f** at  $\delta$  84.0 indicated that this residue was 4-substituted, and consequently corresponded to the  $[\rightarrow 4)\text{-}\beta\text{-D-GlcpA}-(1\rightarrow]$  unit identified by PMAA analy-

Residue	<sup>1</sup> H/ <sup>13</sup> C						
	1	2	3	4	5	6	6'
<b>a</b>	5.32	3.87	3.95	4.14			
→4)-α-D-Galp	95.1	71.3	73.8	81.0			
<b>b</b>	5.26	4.64	4.23	4.56	4.75		
→3)-α-D-GalpA-(2SO <sub>3</sub> <sup>−</sup> )-(1→	101.0	77.6	80.0	73.3	74.6		
<b>c</b>	5.26	4.75	4.30	4.69			
→3,4)-α-D-GalpA-(2SO <sub>3</sub> <sup>−</sup> )-(1→	101.1	77.6	80.0	81.5			
<b>d</b>	5.03	4.17	4.18	4.68	4.83		
→3,4)-α-D-GalpA-(1→	102.4	70.7	82.6	81.3	75		
<b>e</b>	5.03	4.03	4.13	4.52	4.84		
→3)-α-D-GalpA-(1→	102.4	70.7	82.4	73.3	75		
<b>f</b>	~4.75	3.46	3.66	3.77	3.88		
→4)-β-D-GlcpA-(1→	106.3	76.0	77.3	84.0	78.8	178.1	
<b>g</b>	4.73	3.25	3.52	3.31	3.35	3.82	3.59
β-D-Glcp-(1→	106.0	76.8	78.5	73.0	78.5	64.0	
<b>h</b>	4.65	3.56	3.73	4.08			
→4)-β-D-Galp	99.3	74.8	75.7	79.2			
<b>i</b>	4.52	3.34	3.52	3.50	3.76		
β-D-GlcpA-(1→	105.3	75.9	78.5	74.7	78.8	178.6	

Glycosyl sequence information was obtained from ROESY and HMBC experiments. The HMBC spectrum showed an inter-residue correlation between H-1 of **g** ( $\delta$  4.73) and C-4 of **d** ( $\delta$  81.3), which demonstrated that **g** was linked to the 4-position of **d**. Correlation between H-1 of **f** ( $\delta$  4.75) and C-3 of **d** or **e** ( $\delta$  82.6; 82.4) confirmed the presence of the sequence [ $\rightarrow$ 4)- $\beta$ -D-Glc*p*A-(1 $\rightarrow$ 3)- $\alpha$ -D-Gal*p*A-(1 $\rightarrow$ ]. The correlations between the anomeric proton and carbon of **i** and the C-4 and H-4 of **f**, respectively, indicated that **i** was linked to the 4-position of **f**. Correlations between H-1 ( $\delta$  5.03) of **d** and/or **e** and the C-4 of **h** confirmed the link between **d** or **e** and **h** [ $\alpha$ -D-Gal*p*A-(1 $\rightarrow$ 4)-Gal*p*]. These results were confirmed by the ROESY correlations. Inter-residue correlations between H-3 of **d** and H-1 of **f** ( $\delta$  4.75) indicated that **f** was linked to the 3-position of the  $\alpha$ -D-Gal*p*A residue. The correlations between H-1 of **i** and H-4 of **f** proved that **i** was linked to the 4-position of **f**. Therefore, the structures of the tetrasaccharides and the pentasaccharides were identified as in [Chart 1](#). The NMR data are in good agreement with



those reported for a similar EPS produced by another deep-sea bacterium of the same genus, *A. macleodii*.<sup>1</sup>

**2.3.1. Preparation, composition and methylation analysis.** A relatively homogeneous fraction of quite low molecular weight (22,600 g/mol) with a polydispersity of 3.5, was obtained from the native EPS by very mild acid hydrolysis, ultrafiltration and size-exclusion

chromatography and was named LMW-EPS. GLC analysis of the per-*O*-trimethylsilylated methyl glycosides revealed that this fraction was composed of glucose, galactose, glucuronic acid and galacturonic acid with only traces of rhamnose. Sulfate (SO<sub>3</sub>Na, 10%) was also present. Rhamnose was identified in several other fractions representing only a small part of the eluted material and showing 1D NMR spectra very different from the LMW-EPS fraction (results not shown, see also Section 3). This confirmed that the crude EPS contained two polysaccharides, inseparable in the native form, one containing Rha and the other not. Methylation analysis of LMW-EPS indicated the presence of ten different residues (Table 1): glucose (accounting for at least two residues according to the peak intensity) and galactose in terminal position, four monosubstituted and three disubstituted residues [ $\rightarrow$ 2,4)- $\beta$ -D-GlcpA-(1 $\rightarrow$ ]; [ $\rightarrow$ 3,4)- $\beta$ -D-GlcpA-(1 $\rightarrow$ ] and [ $\rightarrow$ 3,4)- $\alpha$ -D-GalpA-(1 $\rightarrow$ ]. This showed the existence of three branching points in the repeating unit.

**2.3.2. NMR studies of LMW-EPS.** The <sup>1</sup>H NMR spectrum of fraction LMW-EPS showed clearly six different low-field signals between 5.1 and 5.6 ppm and an unre-

solved signal (4.5–4.9 ppm, accounting for seven protons) corresponding to H-1 of  $\alpha$ - and  $\beta$ -linked sugars, respectively. The HSQC spectrum clearly allowed the identification of anomeric carbons corresponding to  $\alpha$ -anomeric residues ( $\delta$  100–103) named **A–F** (Table 4). However, in the same spectrum for the 4.5–4.9 cluster, only four H-1/C-1 cross-peaks corresponded to  $\beta$ -anomeric positions, which indicated that three protons in the region between 4.5 and 4.9 were not anomeric. The  $\beta$ -residues were named **K–N** (Table 4).

Most of the signals were assigned after interpretation of DQF-COSY, TOCSY, ROESY, HSQC and HMBC spectra. The chemical shifts are given in Table 4. In the <sup>1</sup>H NMR spectrum, H-1 of **A** resulted from the juxtaposition of three doublets. However, the TOCSY spectrum (Fig. 3) showed that all the H-2, H-3, H-4 and H-5 displayed exactly the same chemical shifts, which showed that **A** was in three similar nearest environments differing only in the vicinity of the H-1. This was due to the heterogeneity generated by the loss of some terminal sugars (see below). The  $\alpha$ -galacto configuration was deduced from the downfield resonance of H-2 and H-3. Carbon chemical shifts were consistent with no substitution at any of the 2, 3 and 4 positions. Residue **B** was

**Table 4.** Chemical shifts ( $\delta$ , ppm) of <sup>1</sup>H and <sup>13</sup>C for the LMW-EPS fraction

Residue	<sup>1</sup> H/ <sup>13</sup> C					
	1	2	3	4	5	6
<b>A</b> $\rightarrow$ 6)- $\alpha$ -D-Galp-(1 $\rightarrow$	5.49–5.57 100.8	3.79 71.3 <sup>a</sup>	3.88 71.5	4.03 72.3	4.12 73.5	4.12 69.3
<b>B</b> $\rightarrow$ 4)- $\alpha$ -D-Galp-(1 $\rightarrow$	5.40 102.8	3.86 71.8	3.93 71.5	4.13 81.8	4.67? —	— —
<b>C</b> $\alpha$ -D-Glcp-(1 $\rightarrow$	5.32 102.1	3.50 75.0 <sup>b</sup>	3.74 75.6	3.46 72.2 <sup>b</sup>	4.00 74.7	— —
<b>D</b> $\rightarrow$ 3,4)- $\alpha$ -D-GalpA-(2SO <sub>3</sub> <sup>−</sup> )-(1 $\rightarrow$	5.26 101.2	4.73 76.9	4.25 80.0	4.68 81.5	~4.7 74.6	— 177.6
<b>E (C)</b> $\alpha$ -D-Glcp-(1 $\rightarrow$	5.24 101.6	3.52 —	3.77 —	3.45 —	3.99 —	— —
<b>F</b> $\alpha$ -D-Glcp-(1 $\rightarrow$	5.20 102.8	3.47 74.8 <sup>b</sup>	3.78 76.1 <sup>a</sup>	3.47 72.2 <sup>b</sup>	4.00 74.7	— —
<b>K</b> 4 $\rightarrow$ )- $\beta$ -D-Glcp-(1 $\rightarrow$	4.73 105.4	3.31 76.1	3.78 76.1	3.55 80.5	3.48 74.9 <sup>b</sup>	— —
<b>L</b> $\beta$ -D-Glcp-(1 $\rightarrow$	4.64 103.2	3.33 76.1	3.78 —	3.86 —	— —	— —
<b>M</b> 2,4 $\rightarrow$ )- $\beta$ -D-GlcpA-(1 $\rightarrow$	4.66 102.9	3.44 82.8	3.76 ~79	3.86 ~79	— —	— 180.0
<b>N</b> 3,4 $\rightarrow$ )- $\beta$ -D-GlcpA-(1 $\rightarrow$	4.67 106.8	3.53 ~75	3.78 83.0	4.05 80.5	3.91 79.7	— 180.0

<sup>a</sup> These attributions could be interchanged.

<sup>b</sup> Idem.



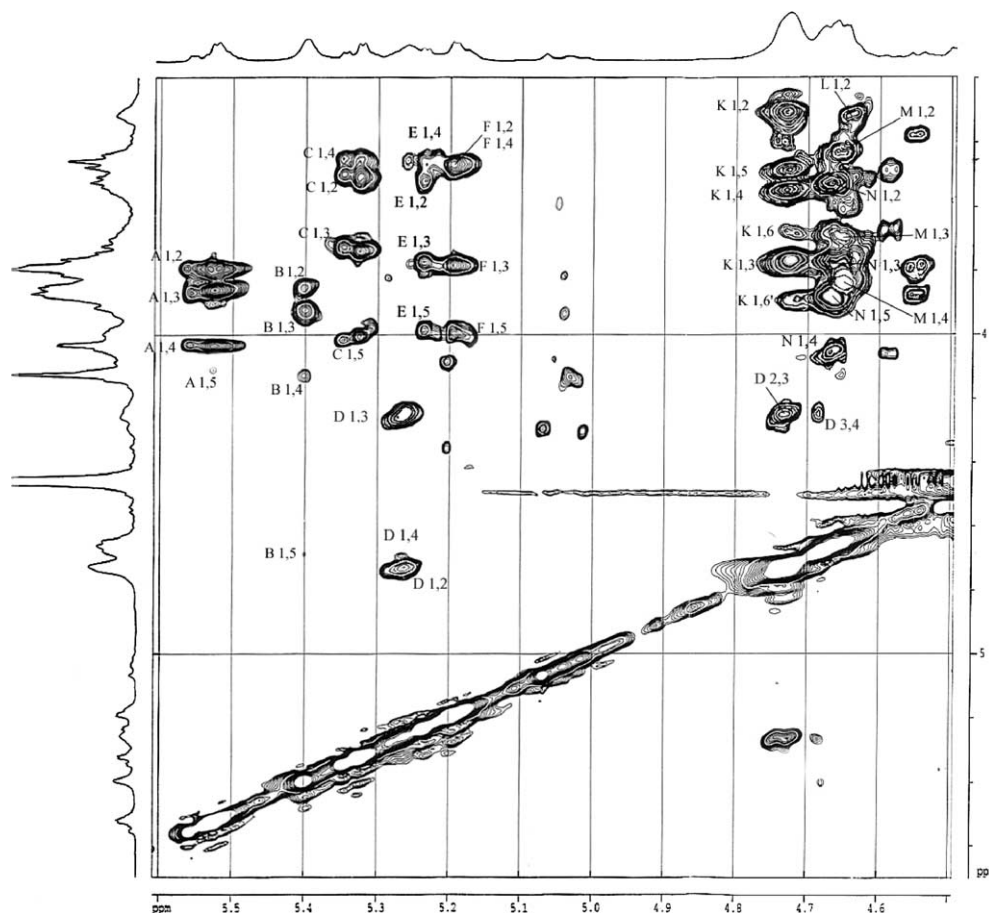


Figure 3. TOCSY spectrum (500 MHz, anomeric region) of LMW-EPS recorded at 325 K in deuterium oxide.

also identified as a  $\alpha$ -D-Galp residue, but the downfield shift of C-4 at  $\delta$  81.8 indicated that it was 4-substituted. Residue **D** was very similar to residue **c** previously described in the OF sample (see Section 2.2) and characterized as a 3,4-disubstituted- $\alpha$ -D-GalpA-[2-SO<sub>3</sub>Na]. The chemical shifts of H-2, H-3, H-4 and H-5 of residues **C**, **E** and **F** were very similar (see TOCSY spectrum) and in agreement with their assignment as residues with an  $\alpha$ -gluco configuration. In addition, H-1 of **C** and **F** appeared as two close doublets, which meant that **C** and **F** were settled in two different, but very similar, environments. On the other hand, H-1 of **E** accounted for less than one proton. For all of these residues (**C**, **E** and **F**) no downfield location of carbon was detected so they were identified as terminal  $\alpha$ -D-Glcp.

Chemical shifts of H-1, H-2 and H-3 of residues **K** and **L** were very similar and consistent with a  $\beta$ -gluco configuration. The downfield shift of C-4 of **K** ( $\delta$  80.5) indicated that this residue was a 4-substituted-Glcp. The signal of the H-1 of **L** ( $\delta$  4.64) was close to H-1 of **M** ( $\delta$  4.66) and **N** ( $\delta$  4.67) and consequently impossible to estimate, but the integration of H-2 of **L** and **K** together represented 1.5 protons, consequently **L** was a residue partially eliminated during the hydrolysis step. Cross-

peaks identified in the HMBC spectrum, between H-4 of residues **M** and **N** and low-field signals ( $\delta$  180.0), indicated that these residues were  $\beta$ -D-glucuronic acid residues. Compounds **M** and **N** could, therefore, be assigned, respectively, to the [ $\rightarrow$ 2,4)- $\beta$ -D-GlcpA] and the [ $\rightarrow$ 3,4)- $\beta$ -D-GlcpA] as supported by the downfield positions of C-2 ( $\delta$  82.8) and C-4 ( $\delta$  79) of **M** and C-3 ( $\delta$  83.0) and C-4 ( $\delta$  80.5) of **N**.

The glycosyl sequence was obtained from HMBC and ROESY (Table 5) experiments. The HMBC spectrum showed correlations proving that the main chain of this EPS was constituted by the trisaccharide **K–D–B** (corresponding to **g–c–a** in the pentasaccharide) and that the sulfated pentasaccharide [**g–c–(f–i)–a**] was contained in the LMW-EPS [**K–D–(N–M)–B**]. The positions of the last four residues (**C**, **F**, **A** and **L**) had to be determined. The observed correlations between **C** and **N** in one hand and between **F** and **M** on the other hand showed that **C** and **F** were linked to **N** and **M**, respectively, as shown in Chart 2. This result was in agreement with the presence of [ $\rightarrow$ 3,4)- $\beta$ -D-GlcpA-(1 $\rightarrow$ )] and [ $\rightarrow$ 2,4)- $\beta$ -D-GlcpA-( $\rightarrow$ )] as deduced from the methylation analysis. The chemical shift of the C-4 of **M** ( $\delta$  79) and the correlation with the H-1 of **A** ( $\delta$  5.53) indicated a  $\alpha$ -(1 $\rightarrow$ 4) linkage

**Table 5.** Correlations observed in the ROESY and HMBC spectra for the LMW-EPS fraction; in the ROESY spectrum between anomeric <sup>1</sup>H and other <sup>1</sup>H; in the HMBC spectrum between anomeric protons and ring carbons and between anomeric carbons and ring protons

Residue ( <sup>1</sup> H-1 δ <sub>H</sub> ) ( <sup>13</sup> C-1 δ <sub>C</sub> )	Linkage	Correlations <sup>1</sup> H-1/ <sup>1</sup> H (ROESY) δ <sub>H</sub> ppm		Long range Correlations <sup>1</sup> H-1/ <sup>13</sup> C (HMBC) δ <sub>l</sub> ppm		Long range Correlations <sup>13</sup> C-1/ <sup>1</sup> H (HMBC) δ <sub>H</sub> ppm	
<b>A</b> δ 5.53 δ 100.8	<b>A</b> (1→4) <b>M</b>	3.79	<b>A</b> , H-2 and <b>M</b> , H-3	71.3	<b>A</b> , C-2	3.86	<b>M</b> , H-4 or <b>A</b> , H-3
		3.86	<b>M</b> , H-4	78.9	<b>M</b> , C-4		
<b>B</b> δ 5.40 δ 102.8	<b>B</b> (1→4) <b>K</b>	3.86	<b>B</b> , H-2	71.8	<b>B</b> , C-3	3.55	<b>K</b> , H-4
		3.93	<b>B</b> , H-3				
		3.48	<b>K</b> , H-5	80.5	<b>K</b> , C-4		
		3.55	<b>K</b> , H-4				
		3.78	<b>K</b> , H-3				
<b>C</b> δ 5.32 δ 102.1	<b>C</b> (1→3) <b>N</b>	3.50	<b>C</b> , H-2 and <b>N</b> , H-2	75.6	<b>C</b> , C-3	3.78	<b>N</b> , H-3
				74.7	<b>C</b> , C-5		
		3.78	<b>N</b> , H-3	83.0	<b>N</b> , C-3		
		3.91	<b>N</b> , H-5				
		4.05	<b>N</b> , H-4				
<b>D</b> δ 5.26 δ 101.2	<b>D</b> (1→4) <b>B</b>	4.73	<b>D</b> , H-2	81.8	<b>B</b> , C-4	4.13	<b>B</b> , H-4
		3.93	<b>B</b> , H-3				
		4.13	<b>B</b> , H-4				
<b>F</b> δ 5.20 δ 102.8	<b>F</b> (1→2) <b>M</b>	3.44	<b>M</b> , H-2	76.1	<b>F</b> , C-3	3.44	<b>M</b> , H-2
		3.77	<b>F</b> , H-3 and <b>M</b> , H-3	74.8	<b>F</b> , C-2 or C-5		
		3.86	<b>M</b> , H-4	82.8	<b>M</b> , C-2		
<b>K</b> δ 4.73 δ 105.4	<b>K</b> (1→4) <b>D</b>	3.31	<b>K</b> , H-2	81.5	<b>D</b> , C-4	4.68	<b>D</b> , H-4
		3.48	<b>K</b> , H-5				
		3.78	<b>K</b> , H-3				
		4.25	<b>D</b> , H-3				
		4.68	<b>D</b> , H-4				
<b>M</b> δ 4.66 δ 102.9	<b>M</b> (1→4) <b>N</b>	3.44	<b>M</b> , H-2	80.5	<b>N</b> , C-4	4.05	<b>N</b> , H-4
		3.78	<b>N</b> , H-3				
		4.05	<b>N</b> , H-4				
<b>N</b> δ 4.67 δ 106.8	<b>N</b> (1→3) <b>D</b>	3.53	<b>N</b> , H-2	80.0	<b>D</b> , C-3	4.25	<b>D</b> , H-3
		3.91	<b>N</b> , H-5				
		4.25	<b>D</b> , H-3				

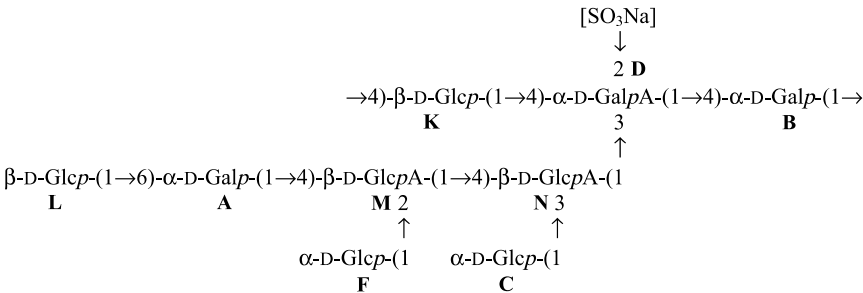


**Chart 2.** Structure of the repeating unit of the *A. infernus* polysaccharide.

between **A** and residue **M**. Positioning the last residue **L** was a little less straightforward. The <sup>13</sup>C signal at 69.3ppm was due to a substituted methylene group according to the DEPT <sup>13</sup>C spectrum while the corre-

sponding <sup>1</sup>H signal (observed in HSQC) was at 4.12ppm. This chemical shift corresponded to H-5 of **A** and H-4 of **B** but also to H-6 of **A**, therefore **A** was 6-substituted. In addition, in the HMBC spectrum, the



proton resonance at 4.12 ppm was connected to C-1 of **D** (because of the link between **D** and **B**) and to C-1 of **L** (although weakly). Consequently, the last residue **L**, corresponding to less than one residue (probably because **L** was easily removed), was bound to the position 6 of **A**. Methylation analysis sustained this result because the [ $\rightarrow$ 6)-Galp-(1 $\rightarrow$ )] residue was detected in low quantities in LMW-EPS but in higher quantities in the native EPS. Terminal residues (**L**, **C** and **F**) were indeed partially removed, which explained the presence of relatively large quantities of terminal Gal and [ $\rightarrow$ 4)-Glc pA-(1 $\rightarrow$ )] in PMAA analysis and which also generated the already noticed heterogeneity for H-1 of residues **A**, **C** and **F**. The presence of **E** could be explained in a similar way. Obviously some desulfation also occurred, H-1 of **C** was probably close to the sulfate group of **D** (according to Dreiding models) and consequently appeared at low field ( $\delta$  5.32), when the sulfate was removed that generated a new residue **E** differing from **C** only by its H-1 chemical shift ( $\delta$  5.24, see Table 4). Additional evidence showing that **E** was generated from **C** by desulfation of **D** is that **E** was undetectable in the LMW-EPS sample obtained by a free radical depolymerization process<sup>7</sup> causing no desulfation. Thus, the structure of the repeating unit of the *A. infernus* polysaccharide can be written as in Chart 2.

As already noticed, the backbone of this polysaccharide displays some similarities to that described for the EPS of *A. macleodii*.<sup>1</sup> This is not surprising since both strains belong to the *Alteromonas* genus and were collected in similar environments. At the same time, *A. infernus* EPS differs inter alia by its exceptionally crowded GalA and by its very uncommon disubstituted side chain. The knowledge of its structure will allow this molecule to be modified more rationally in order to prepare well-characterized oligosaccharides as required for medicinal use.

### 3. Experimental

#### 3.1. Production and purification of native exopolysaccharides

The isolation procedure and characteristics of the GY785 strain have previously been reported.<sup>5</sup> EPS was produced and purified as previously described.<sup>6</sup>

#### 3.2. Preparation of partially hydrolyzed exopolysaccharides (LMW-EPS)

Crude EPS was dissolved in 1 M H<sub>2</sub>SO<sub>4</sub> at 5 g/L and heated at 60°C for 90 min. The preparation was then neutralized with a solution of 1 M NaOH, ultrafiltered (1000 Da cut-off membrane) to eliminate salts and small oligosaccharides and finally freeze dried. 1D NMR spec-

trum of this crude LMW-EPS was recorded. This material (40 mg) was then dissolved in 0.1 M ammonium bicarbonate and applied to a size-exclusion chromatographic column (40  $\times$  4.8 cm) of Sephacryl HR (Pharmacia) and eluted with the same buffer. Detection was performed using a refractometer (Gilson), eluted material was collected in 19 fractions of 50 mL. An aliquot of each fraction was taken out and corresponding 1D NMR spectra were recorded. Fractions 10, 11 and 12 were pooled and named LMW-EPS, because they displayed almost identical spectra similar to this of the crude hydrolysate, but without the Me signal due to Rha. The Rha-containing fractions were eluted early and showed very different NMR spectra. Then the pooled fractions were applied to a cation exchange chromatographic column (45  $\times$  1.5 cm) of Dowex HCR-S/Na<sup>+</sup> form. Elution was performed using water and the polysaccharide fractions were freeze dried. The molecular weight of this LMW-EPS was determined as previously described by high-performance size-exclusion chromatography (HPSEC) using pullulan as standard.<sup>7</sup> Pullulan is a neutral glucan, whereas LMW-EPS is highly negatively charged polysaccharide. Consequently, such a calibration, which does not allow an exact measure of molecular mass, was used only for having a rough estimation of MW and homogeneity.

#### 3.3. Preparation of the oligosaccharide fraction (OF)

An oligosaccharide preparation was obtained from the crude EPS dissolved in 1 M H<sub>2</sub>SO<sub>4</sub> at 2 g/L and heated at 85°C for 210 min. After cooling at room temperature, calcium carbonate was added to obtain a final pH of 7 and the solution was filtered. It was then ultrafiltered (1000 Da cut-off membrane), converted to sodium salt using cation exchange chromatography as described above and finally freeze dried. An aliquot was reduced by NaBH<sub>4</sub>.

#### 3.4. Sulfate content

Elemental analysis was performed by the Central Microanalysis Department of the CNRS (Gif/Yvette, France). Sulfate content (sodium salt) was calculated from sulfur analysis according to the following relation: sulfate group =  $3.22 \times \text{S}\%$ .

#### 3.5. Constituent analysis

Monosaccharide content was determined after methanolysis by gas chromatography.<sup>2</sup> Methanolysis was performed in 2 M MeOH-HCl at 100°C for 4 h, and the resulting methylglycosides were converted to the corresponding trimethylsilyl derivatives as described by Montreuil et al.<sup>10</sup> Separation and quantification of the per-*O*-trimethylsilyl methyl glycosides was performed

on a 5890 series II (Hewlett–Packard) system with FID detection, using a Chrompack CPSil-5CB fused-silica column (0.25 mm  $\times$  50 m) and a temperature program of 50–120 °C at 20 °C/min then 120–240 °C at 2 °C/min and finally 240–280 °C at 10 °C/min. The absolute configuration of the sugars was determined by the Gerwig et al. method.<sup>11</sup>

### 3.6. Methylation analysis

Methylation analysis was performed using a modification of the Hakomori procedure.<sup>12</sup> Hydroxyl groups were methylated by methyl iodide in Me<sub>2</sub>SO using lithium dimethylsulfonyl as anion. Methyl esters of uronic acids were reduced by lithium triethylborodeuteride, as previously described.<sup>13</sup> Methylated EPS was then hydrolyzed with 2 M trifluoroacetic acid for 2 h at 120 °C. The derivatives were reduced by NaBD<sub>4</sub> and acetylated with Ac<sub>2</sub>O and 1-methylimidazole prior to analysis by gas chromatography–mass spectrometry (GC/MS)<sup>1</sup> carried out on an HP-5890 system using a DB-1 fused-silica column (0.25 mm  $\times$  30 m) and a temperature program of 140–220 °C at 2 °C/min. Ionization was carried out in electron impact (EI, 70 eV).

### 3.7. Electrospray ionization-mass spectrometry (ESIMS)

ESIMS was run in negative mode using a high-resolution MS/MS spectrometer (Micromass ZABSpecTOF) using 1:1 water–MeCN and NH<sub>3</sub> ( $\approx$ 0.1%, v/v) as the mobile phase.

### 3.8. NMR studies

NMR spectra were recorded at 298 or 325 K on a solution of polysaccharide in D<sub>2</sub>O on Bruker DRX-400 and AMX 500 spectrometers using UXNMR software. Double-quantum filtered <sup>1</sup>H–<sup>1</sup>H correlated spectroscopy (DQF-COSY), total correlation spectroscopy (TOCSY) with a mixing time of 80–100 ms, and heteronuclear single quantum coherence (HSQC) were performed according to standard pulse sequences. For inter-residue correlation, two-dimensional Rotating-frame Overhauser Enhancement Spectroscopy (ROESY) experiment, with a mixing time of 350 ms and heteronuclear multiple bond correlation (HMBC), with a delay of 60 ms, were

used. <sup>1</sup>H and <sup>13</sup>C NMR chemical shifts were expressed in ppm relative to sodium 2,2,3,3-tetradeuterio-4,4-dimethyl-4-silapentanoate.

### Acknowledgements

This work was supported by CNRS and IFREMER. The authors thank Dr. Jean Guezennec for his support in this task, as well as Dr. Jacqueline Jozefonvicz for her interest in this work. They are indebted to Corinne Siquin for preparing raw EPS and the CRMPO for recording the ESIMS spectra. They are grateful to Drs. Barbara Mulloy and Roger Pichon for fruitful discussions about NMR spectra.

### References

1. Rougeaux, H.; Talaga, P.; Carlson, R. W.; Guezennec, J. *Carbohydr. Res.* **1998**, *312*, 53–59.
2. Rougeaux, H.; Kervarec, N.; Pichon, R.; Guezennec, J. *Carbohydr. Res.* **1999**, *322*, 40–45.
3. Vincent, P.; Pignet, P.; Talmont, F.; Bozzi, L.; Fournet, B.; Guezennec, J.; Jeanthon, C.; Prieur, D. *Appl. Environ. Microbiol.* **1994**, *60*, 4134–4141.
4. Loaëc, M.; Olier, R.; Guezennec, J. *Wat. Res.* **1997**, *31*, 1171–1179.
5. Raguénès, G. H.; Peres, A.; Ruimy, R.; Pignet, P.; Christen, R.; Loaëc, M.; Rougeaux, H.; Barbier, G.; Guezennec, J. G. *J. Appl. Microbiol.* **1997**, *82*, 422–430.
6. Guezennec, J.; Pignet, P.; Lijour, Y.; Gentric, E.; Ratiskol, J.; Collic-Jouault, S. *Carbohydr. Polym.* **1998**, *37*, 19–24.
7. Collic-Jouault, S.; Chevolot, L.; Helley, D.; Ratiskol, J.; Bross, A.; Siquin, C.; Roger, O.; Fischer, A. M. *Biochim. Biophys. Acta* **2001**, *1528*, 141–151.
8. Linhardt, R. J.; Desai, U. R.; Liu, J.; Pervin, A.; Hoppensteadt, D.; Fareed, J. *Biochem. Pharmacol.* **1994**, *47*, 1241–1252.
9. Yang, B. Y.; Montgomery, R. *Carbohydr. Res.* **2001**, *332*, 317–323.
10. Montreuil, J.; Bouquelet, S.; Debray, H.; Fournet, B.; Spik, G.; Strecker, G. In *Carbohydrate Analysis: A Practical Approach*; Chaplin, M. F., Kennedy, J. F., Eds.; Oxford University Press: New York, 1986; pp 143–204.
11. Gerwig, G. J.; Kamerling, J. P.; Vliegthart, J. F. G. *Carbohydr. Res.* **1978**, *62*, 349–357.
12. Hakomori, S. *J. Biochem. (Tokyo)* **1964**, *55*, 205–208.
13. York, W. S.; Darvill, A. G.; McNeil, M.; Stevenson, T. T.; Albersheim, P. *Methods Enzymol.* **1985**, *118*, 3–40.